Atmos. Chem. Phys. Discuss., 10, 26473–26512, 2010
www.atmos-chem-phys-discuss.net/10/26473/2010/
doi:10.5194/acpd-10-26473-2010

Atmospheric Chemistry and Physics Discussions

First carbon dioxide atmospheric vertical profiles retrieved from space observation using ACE-FTS solar occultation instrument

P. Y. Foucher[1,2], **A. Chédin**[1], **R. Armante**[1], **C. Boone**[3], **C. Crevoisier**[1], **and P. Bernath**[3,4]

[1]Laboratoire de Météorologie Dynamique/Institut Pierre Simon Laplace, Ecole Polytechnique, UMR 8539, 91128 Palaiseau, France
[2]Onera – Centre Midi Pyrénées, BP74025, 2 Avenue Edouard Belin, 31055 Toulouse Cedex 4, France
[3]Department of Chemistry, University of Waterloo, Ontario, N2L3G1, Canada
[4]Department of Chemistry, University of York, Heslington, York, YO105DD, UK

Received: 9 August 2010 – Accepted: 27 October 2010 – Published: 5 November 2010

Correspondence to: P. Y. Foucher (pierre-yves.foucher@lmd.polytechnique.fr)

Published by Copernicus Publications on behalf of the European Geosciences Union.

Abstract

Major limitations of our present knowledge of the global distribution of CO_2 in the atmosphere are the uncertainty in atmospheric transport and the sparseness of in situ concentration measurements. Limb viewing spaceborne sounders such as the Atmospheric Chemistry Experiment Fourier transform spectrometer (ACE-FTS) offer a vertical resolution of a few kilometres for profiles, which is much better than currently flying or planned nadir sounding instruments can achieve. After having demonstrated the feasibility of obtaining CO_2 vertical profiles in the 5–25 km altitude range with an accuracy of about 2 ppm in a previous study, we present here the results of five years of ACE-FTS observations in terms of monthly mean profiles of CO_2 averaged over 10° latitude bands for northern mid-latitudes. These results are compared with in-situ aircraft measurements and with simulations from two different air transport models. Key features of the measured altitude distribution of CO_2 are shown to be accurately reproduced by the ACE-FTS retrievals: variation in altitude of the seasonal cycle amplitude and extrema, seasonal change of the vertical gradient, and mean growth rate. We show that small but significant differences from model simulations could result from an over estimation of the model circulation strength during the northern hemisphere spring. Coupled with column measurements from a nadir viewing instrument, it is expected that occultation measurements will bring useful constraints to the surface carbon flux determination.

1 Introduction

Determining the spatial and temporal structure of surface carbon fluxes has become a major scientific goal during the last decade. In the so-called "inverse" approach, observed atmospheric concentration gradients are used to disentangle surface fluxes, given some description of atmospheric transport. Major limitations of the inverse approach are the sparseness of atmospheric CO_2 concentration measurements, often

ACPD
10, 26473–26512, 2010

compensated for by introducing questionable constraining conditions, and, more significantly, the uncertainties in atmospheric transport. Since CO_2 is inert in the lower atmosphere, its long-term trend and pronounced seasonal cycle propagate from the surface, and the difference between atmospheric and surface mixing ratios is determined by the processes that transport surface air throughout the atmosphere, including advection, convection and eddy mixing (Shia et al., 2006). Because it takes several months to transport surface air to the lower stratosphere, the CO_2 mixing ratio is lower and the seasonal cycle is different there as compared to the troposphere (Plumb and Ko, 1992; Plumb, 1996; Shia et al., 2006). Bönisch et al. (2008) evaluated transport in three-dimensional chemical transport models in the upper troposphere and lower stratosphere by using observed distributions of CO_2 and SF_6. They show that although all models are able to capture the general features in tracer distributions including the vertical and horizontal propagation of the CO_2 seasonal cycle, important problems remain such as: (i) a too strong Brewer-Dobson circulation (with air rising across the tropical tropopause, moving poleward, and sinking to the extratropical troposphere) causing an overestimate of the tracer concentration in the lower most stratosphere (LMS) during winter and spring and, (ii) a too strong tropical isolation leading to an underestimate of the tracers in the LMS during winter. Moreover, all models tested suffer to some extent from diffusion and/or too strong mixing across the tropopause. In addition, the models show too weak vertical upward transport into the upper troposphere during the boreal summer.

In recent years it has become possible to measure atmospheric CO_2 from space observations by the nadir-viewing thermal infrared vertical sounders such as TIROS-N Operational Vertical Sounder (TOVS) (Chédin et al., 2002, 2003a), Atmospheric Infrared Sounder (AIRS) and Infrared Atmospheric Sounder Interferometer (IASI) (Chédin et al., 2003b; Crevoisier et al., 2004, 2009), or in the near infrared by SCIAMACHY (Buchwitz et al., 2005) and Greenhouse gases Observing SATellite (GOSAT) (Kuze et al., 2009). However, the satellite data products are all vertically integrated concentrations rather than the profile measurements that are essential for a comprehensive

ACPD
10, 26473–26512, 2010

understanding of distribution mechanisms of CO_2. The difference between the column-averaged CO_2 mixing ratio and the surface value varies from 2 to 10 ppm depending on location and time of year (Olsen and Randerson, 2004). The upper troposphere can contribute significantly to this difference because this portion of the column constitutes approximately 20% of the column air mass and the CO_2 mixing ratios in this region can differ by 5 ppm or more from the CO_2 mixing ratios at the surface (Anderson et al., 1996; Matsueda et al., 2002; Shia et al., 2006). With limb sounders that observe the atmosphere along tangential optical paths, the vertical resolution of the measured vertical profiles is of the order of a few kilometres, much better than can be achieved with nadir sounding instruments. The Atmospheric Chemistry Experiment Fourier transform spectrometer (ACE-FTS), launched in August 2003 on board SCISAT, is a limb sounder that records solar occultation measurements (up to 30 occultations each day) with coverage between approximately 85° N and 85° S (Bernath et al., 2005), with more observations at high latitudes than over the tropics (Bernath et al., 2006). The ACE-FTS has high spectral resolution (0.02 cm^{-1}) and the signal-to-noise ratio of ACE-FTS spectra is higher than 300:1 over a large portion (1000–3000 cm^{-1}) of the spectral range covered (750–4400 cm^{-1}). Recently, Foucher et al. (2009) and Foucher (2009) have shown that the ACE-FTS instrument is able to provide CO_2 vertical profiles in the 5–25 km altitude range with an estimated CO_2 total error characterized by a bias of about ±1 ppm and a standard deviation of about 2 ppm after averaging over 20 spatially and temporally consistent retrieved profiles.

Our analysis is organised as follows. We first summarize the main features of the method developed to retrieve CO_2 profiles and describe how ACE-FTS occultations are selected (Sect. 2) and the limits of their spatial and temporal coverage. ACE-retrieved monthly mean CO_2 vertical profiles averaged over the latitude bands 40° N–60° N and 50° N–60° N and covering the 2004–2008 time period are then presented and compared (vertical gradients, seasonal cycles at various altitudes, growth rates) with aircraft in-situ measurements (Sect. 3) and with simulations from two different air transport models (Sect. 4). Section 5 presents our conclusions.

ACPD
10, 26473–26512, 2010

2 Method and ACE-FTS data

The methodology used to determine CO_2 profiles from ACE-FTS observations has been described in detail in Foucher et al. (2009), hereafter referred to as Fal2009, and Foucher (2009). The retrieval process has two main steps: pointing parameter estimation (tangent heights, pressure and temperature profiles) and CO_2 vertical profile estimation. Both steps use a similar constrained least-squares retrieval method. The target variable is a vector containing tangent heights and a temperature profile in the first step or a CO_2 concentration vertical profile in the second step.

2.1 ACE-FTS pointing knowledge

Interpreting limb viewing observations in terms of atmospheric variables requires accurate knowledge of instrument pointing parameters (tangent heights) and pressure/temperature ("pT") vertical profiles. Reactive trace gases are the usual target species of limb-viewing instruments, so pointing parameters are simultaneously retrieved with pT by the analysis of properly selected CO_2 lines under the assumption (questionable, in certain cases) of a weak variation of its atmospheric concentration around a given a priori value. As carbon dioxide is here the target species, a critical step in this research has therefore been to develop a method of obtaining pT profiles and tangent heights independent of any a priori CO_2 knowledge. A new approach based on the N_2 collision-induced continuum absorption near 4.3 µm was presented in Fal2009 together with a new parametric N_2 continuum absorption model (Foucher et al., 2010), derived from Lafferty et al. (1996) laboratory measurements. The high sensitivity of N_2 continuum absorption to altitude affords a precision of better than 50 m in the tangent height retrieval. Figure 1 shows N_2 continuum transmittance sensitivity to tangent height in the 2400–2600 cm^{-1} spectral range. As explained in Fal2009, six optimized microwindows have been selected in the 2400–2500 cm^{-1} wave number range in order to cover the 5–25 km altitude range. In an iterative process using hydrostatic equilibrium we obtain ACE-FTS tangent altitudes independent of a priori CO_2 data with a high precision

ACPD
10, 26473–26512, 2010

(∼ 50 m standard deviation). Finally, empirical corrections are added to these altitudes to account for problems in the transmission model which does not include effects of N_2-H_2O collisions, which are still not accurately known. In addition, although we included the latest developments in the modelling of line wings based on Niro et al. (2004), there might still be uncertainties near 2400 cm^{-1}. These empirical corrections have been estimated based on the analysis of the mean difference between ACE v2.2 tangent heights (Boone et al., 2005) and tangent heights retrieved from the N_2 continuum, based on averages over the entire 2004–2008 time period. This mean bias depends on the altitude and varies from –2.5% at lowest altitude to +2% at 20 km. This correction is applied to all occultations and is described in more detail in Foucher et al. (2009). Using a method similar to that described in Foucher (2009); Rinsland et al. (2010) find ACE-retrieved CO_2 mean tropospheric (7–10 km) concentrations around 405–420 ppm, too high by about 30 ppm. This large bias is likely due to the use of an uncorrected N_2 continuum absorption.

2.2 Selection of ACE-FTS occultations

A high inclination (74°), circular, low Earth orbit (650 km) gives ACE coverage of tropical, mid-latitude and polar regions. The ACE orbit was selected so that the coverage repeats annually in latitude (Bernath et al., 2006) and is optimized for high latitude coverage in both hemispheres. Observations are available since early 2004. To be selected for the CO_2 retrieval process, an ACE-FTS occultation must fulfill two criteria.

First, the occultation must be declared "clear" after having passed a series of tests aiming at detecting the presence of clouds along the optical path. These tests are based on comparisons between clear-sky simulated and measured transmittances. Using a quasi transparent window near 970 cm^{-1} (10.3 µm), an occultation is rejected if the measured transmittance is lower than a fixed value corresponding to the occultation tangent height, these threshold values being determined from simulations. Similar "static" tests are carried out for N_2 microwindows. Then, "dynamic" tests are carried out consisting of comparing changes in transmittance from one measurement to the next.

ACPD
10, 26473–26512, 2010

If the difference is larger than what can be expected from simulations, the occultation is rejected. These dynamic tests use the N_2 microwindows.

Second, the lowest measured tangent height must be less than 12 km as ACE occultations beginning at tangent altitudes higher than 12 km are often characterized by a high probability of instrumental or meteorological anomalies such as clouds. Figure 2 (top) shows the locations of the occultations finally selected for each month of the year 2005 and the monthly distribution of the number of occultations available for 10° latitude bands from 60° N to 60° S for the year 2005. The prevalence of high latitudes is clearly seen in Fig. 2 although some lower latitudes also have a considerable number of occultations as shown in Fig. 2 (bottom). The present analysis of the first ACE-retrieved CO_2 profiles focuses on the 50° N–60° N latitude band which is seen to be the richest band for occultations over non polar regions. Figure 3 shows the number of occultations available per month (y-axis), for each altitude in the range 6–22 km (x-axis), in the 50° N–60° N latitude band and for each year from 2005 to 2007. Available occultations presented in Fig. 2 correspond to about 50% of the total number of ACE occultations. This figure shows a substantial variability in altitude and month as well as in time. As already seen in Fig. 2 for this latitude band, some months are not covered at all (April, August, and October). However, for the nine other months, results must be interpreted carefully when the number of occultations available is significantly less than 20. This is the case below 8 km most of the time. This is also the case for February, June and September in 2007 at all altitudes for this latitude band and for other year/months. The year 2005 shows the largest number of months with more than 20 occultations available for a relatively large number of altitudes (about 6 months); 2006 and 2007 only show 4 such months.

2.3 CO_2 profile retrieval

The method used to determine CO_2 profiles from ACE-FTS observations has been described in Fal2009. The CO_2 microwindow optimized selection is composed of two sets, one dedicated to the 5–15 km altitude range using the $^{18}OC^{16}O$ isotopologue

ACPD
10, 26473–26512, 2010

and the other dedicated to the 10–25 km altitude range using the main isotopologue $^{12}C^{16}O_2$. In each case, about 15 microwindows with a spectral width of 0.2 to 0.5 cm^{-1} (located around 1900, 2600 and 3000 cm^{-1}) have been selected from a larger set of more than 80 microwindows given in Foucher (2009). As shown in this reference, increasing the number of microwindows used for the retrieval decreases the instrumental noise error but, at the same time, may increases errors due to uncertainties in temperature and other interfering species. We have shown that the mean error due to all sources of uncertainties decreases from 10 ppm using only one microwindow to 3 ppm using 15 microwindows. An altitude dependent regularization matrix has been used based on a 1st order Tikhonov regularization matrix (Tikhonov, 1963) weighted by a priori knowledge of CO_2 variance from the MOZART chemistry and transport model (Horowitz et al., 2003). The forward solution of the radiative transfer equation is provided by the 4A/OP-limb Radiative Transfer Model. 4A (for Automatized Atmospheric Absorption Atlas) is a fast and accurate line-by-line radiative transfer model (Scott and Chédin, 1981) developed and maintained at Laboratoire de Météorologie Dynamique (LMD; see http://ara.lmd.polytechnique.fr) and was made operational (OP) in cooperation with the French company Noveltis (see http://www.noveltis.fr/4AOP/ for a description of the 4A/OP version).

Figure 4 shows results from realistic simulations of retrieved CO_2 mixing ratio profiles averaged over 20 occultations. In the first case (blue curves), all uncertainties (temperature, instrument, interfering species, etc.) are considered as spectrally independent and translated into an equivalent Gaussian random noise. This equivalent noise corresponds to around 4 times the signal to noise ratio in the analyzed transmittance spectra, that is to say 1%. In the second case (red curves), uncertainties are introduced directly in the description of the atmosphere of each retrieval, temperature (2 K standard deviation) and interfering species concentration (10% standard deviation), prior to simulating "observed" transmittances. In the second case, more realistic, the mean retrieval bias after averaging over 20 occultations is around 1 ppm with a standard deviation of about 3–4 ppm, and decreases for increasing altitudes (see Fal2009). Results from a detailed

ACPD
10, 26473–26512, 2010

analysis of the retrieval process presented in Fal2009 have demonstrated a mean vertical resolution of about 2.5 km. This is summarized on Fig. 4 which shows examples of averaging kernels for levels at 6, 8, 10 12 and 14 km for one occultation. Each averaging kernel represents the sensitivity of the CO_2 value retrieved at this level with respect to a change in the true profile, its full width at half maximum corresponds to the vertical resolution. The blue curves correspond to the altitude dependent regularisation used here. In this case, we can estimate that the vertical resolution is around 2 km for the lowest altitudes and about 2.5 km at 15 km. The estimated CO_2 total error is characterized by a bias of about ±1 ppm and a standard deviation of about 2 ppm after averaging over 20 spatially and temporally consistent profiles (Fal2009). Averaging over less occultations may increases the total error, and is the reason why the minimum number of occultations has been set to 5, corresponding to a mean standard deviation of about 5 ppm.

At present, five years (2004–2008) of ACE-FTS observations have been processed using the method briefly described above and provide, for the first time, CO_2 vertical profiles on a near global scale. Here, we focus on the time period 2004–2008 and the latitude bands 40° N–60° N and 50° N–60° N that are well covered by ACE and for which in situ aircraft measurements of CO_2 are available. For each month we obtain a mean profile covering the 10–25 km range using lines from the main CO_2 isotopologue, as well as a mean profile covering the 5–15 km range using lines from the $^{18}OC^{16}O$ isotopologue: the $^{18}OC^{16}O$ isotopologue lines are employed because the main isotopologue lines become saturated at low altitude. As shown by Boone et al. (2005), we can expect an overestimation of 3.5% of the CO_2 concentration retrieved from the $^{18}OC^{16}O$ isotopologue due to either errors in the strengths of the $^{18}OC^{16}O$ lines in the line list (here "GEISA", Jacquinet-Husson et al., 2008) and/or to a difference in the mixing ratios from the expected $^{18}OC^{16}O/^{12}C^{16}O_2$ isotopic ratio. For each occultation, we estimate the ratio between CO_2 concentrations retrieved from the $^{18}OC^{16}O$ isotopologue lines and $^{12}C^{16}O_2$ main isotopologue lines in the overlap region, between 10 and 15 km. This ratio is then applied to the entire $^{18}OC^{16}O$ isotopologue

ACPD
10, 26473–26512, 2010

profile to build a unique profile from 5 to 25 km. The mean ratio measured is about 2.5% in the 40–60° N latitude band, a value close to the 3.5% global mean value estimated by Boone et al. (2005). Finally, we apply a linear filter (Eq. 1), to smooth the final retrieved profile on the 1 km grid with a minor impact on the 2.5 km mean vertical resolution.

$$CO_{2final}(z) = 0.25CO_2(z+1) + 0.5CO_2(z) + 0.25CO_2(z-1), \quad (1)$$

z is the 1 km grid level.

Averaged over the 2004–2006 time period, separately for each isotopologue, the CO_2 profile monthly mean standard deviations (std), which result from both errors in the method and variability of the CO_2 concentrations over one month in the latitude band considered (here 50° N–60° N), vary with altitude and month. Smallest values, of the order of 2 ppm or less, are observed between 12–13 km and 24 km in May–July and, to a lesser extent, September. Above 22 km, std values may reach 4 ppm in December–February, with a peak at 5 ppm at 24 km in February. Below 12–13 km, std values, as expected from the greater natural variability of the CO_2 seasonal cycle at lower altitudes, are more variable. For most of the months, the std fluctuates around 3 ppm (±1 ppm) with larger values for $^{18}OC^{16}O$, in particular at 10 and/or 11 km. At these altitudes, the main isotopologue generally shows lower std values. Below 10 km, where results come exclusively from the $^{18}OC^{16}O$ isotopologue and fewer occultations contribute to the average, std values are below 4 ppm except for a peak of almost 6 ppm in March.

3 Comparisons with aircraft in-situ measurements time-series

Commercial aircraft-based observations using in situ measurement systems have made significant contributions to our present knowledge of the distribution of CO_2 in the atmosphere. Major contributions include measurements of CO_2 over Japan and the western Pacific (Nakazawa et al., 1991; Matsueda et al., 2002; Machida et al., 2008; Matsueda et al., 2008), in particular with the ongoing CONTRAIL program. From Europe to

ACPD
10, 26473–26512, 2010

the tropics measurements have been made available from the Civil Aircraft for the Regular Investigation of the Atmosphere Based on an Instrument Container (CARIBIC; Brenninkmeijer et al., 1999, 2007) program and from the SPURT (Spurenstofftransport in der Tropopausenregion/trace gas transport in the tropopause region) campaigns in Europe (Hoor et al., 2004; Engel et al., 2006; Bönisch et al., 2008; Gurk et al., 2008). This section presents comparisons between ACE-FTS CO_2 profiles and these in situ observations.

3.1 CO_2 in the upper troposphere (9–10 km)

ACE-retrieved upper tropospheric CO_2 concentrations are first compared to results from the CARIBIC experiment as given in Schuck et al. (2009). These upper troposphere CO_2 monthly mean concentration time series correspond to flights to Asia covering the latitudes from about 20° N to about 55° N and are compared in Fig. 5 to ACE monthly mean retrieved concentrations for the 40° N–60° N latitude band. A relatively good agreement is seen between the two sets of CO_2 concentrations: the mean difference between the two polynomial fits (each fit uses a linear trend and two harmonics) to either the measurements or to the retrievals (Schuck et al., 2009) is less than 2 ppm. However, a temporal shift is observed between the two curves, with the ACE-FTS peaking about one month earlier than CARIBIC. We see two possible reasons for this difference: (i) the fact that CARIBIC covers latitudes that are on average smaller than ACE (the 40° N–60° N latitude band has been chosen to obtain as many non-polar occultations as possible) for which the peak is expected earlier, and, (ii) the difficulty in correctly positioning the minimum month because of the absence of ACE data for the months of August and October. The slopes of the best fit lines also agree and correspond to a mean tropospheric annual growth rate of about 1.9 ppm yr^{-1} from 2005 to 2008, in agreement with the mean annual growth rate observed at the surface for this time period (see, for example, http://www.esrl.noaa.gov/gmd/ccgg/trends/).

ACPD
10, 26473–26512, 2010

3.2 CO_2 below, around, and above the tropopause: from 8–9 km to 16–18 km

Figure 6 (top), which is similar to Fig. 5 but for the 50° N–60° N latitude band and the 2004–2008 time period, displays time series of ACE-retrieved monthly mean CO_2 concentrations for six atmospheric layers: 8–9 km, 9–10 km, 10–12 km, 11–13 km, 12–14 km, and 16–18 km, spanning the upper troposphere to the lower stratosphere. Monthly mean retrieved concentrations are represented by crosses and the curves result from the harmonic polynomial fit (two harmonics for the first two layers, one harmonic for the remaining four) to the retrievals at different altitudes. Figure 6 (bottom), from Sawa et al. (2008), also displays CONTRAIL CO_2 time series measurements above Eurasia in a similar altitude range from November 2005 to September 2007. Figure 6 (top) can also be directly compared to results from SPURT (see Fig. 9 of Hoor et al., 2004 and Fig. 5 of Gurk et al., 2008). ACE-retrieved CO_2 vertical profiles, SPURT and CONTRAIL in situ measurements show key features of the CO_2 distribution with altitude. First, the amplitude of the CO_2 tropospheric seasonal cycle (detrended) decreases from 7–8 ppm below the tropopause at 9–10 km to ∼1–2 ppm at 10–12 km and the amplitude increases again in the stratosphere at 16–18 km, in agreement with the observations but with an amplitude (2–3 ppm) somewhat too large for the highest layer. As pointed out by Hoor et al. (2004), the phase of the cycle remains tropospheric with a minimum in summer up to the lowermost stratosphere at 10–12 km, reflecting the strong coupling between the lowermost stratosphere and the extra-tropical troposphere through troposphere to stratosphere transport of air that entered the stratosphere at the tropical tropopause. The dampening of the amplitude of the seasonal cycle reflects the role of the extratropical tropopause as a barrier to transport (Hoor et al., 2004). Above, the phase maximum is shifted by up to three months towards summer as observed in-situ. Second, a negative vertical gradient is clearly seen on Fig. 6 in August which accurately reproduces the negative gradient seen by SPURT and by CONTRAIL. This leads to a significant vertical gradient during winter and spring, and to a very weak gradient (sometimes positive) from 9 to 18 km in summer and fall. Third, at all altitudes

ACPD
10, 26473–26512, 2010

the CO_2 concentration exhibits a mean temporal trend of about 1.9 ppm yr^{-1}, again in good agreement with the mean annual growth rate observed at the surface for this time period. These comparisons show that the CO_2 concentrations retrieved from ACE-FTS are consistent with aircraft in situ measurements in the Northern Hemisphere mid-latitudes. In particular, the mean growth rate, the seasonal vertical gradient change and phase shift from the mid-troposphere to the lower stratosphere are well represented by ACE-retrieved CO_2 values. However the stratosphere seasonal cycle amplitude seems to be over-estimated. A possible explanation could come from the difference in the spatial coverage of the different data sets. Indeed, ACE-FTS results sum all latitudes and longitudes in the 50° N–60° N band, whereas SPURT, CARIBIC, and CONTRAIL data correspond to observations above Europe, Eurasia, and Asia, respectively.

4 Comparisons with air-transport model CO_2 profiles

Another way of assessing the quality of the ACE-retrieved CO_2 vertical profiles is to compare them with air transport model simulations. For that purpose, two well known models have been used. First, we consider the Flexpart Lagrangian particulate dispersion model (Stohl et al., 2005) driven with meteorological input data (wind, temperature and humidity fields) from the European Centre for Medium Range Weather Forecasts (ECMWF). CO_2 surface data from the World Data Centre for Greenhouse Gases (WDCGG, http://gaw.kishou.go.jp/wdcgg) have been used to create a source function for the lower most troposphere. CO_2 fields from a six-year analysis have been monthly averaged for 10° latitude bands to make comparisons with profiles retrieved from ACE-FTS for the year 2006. The second model considered generates CO_2 model simulations from the CarbonTracker (2009, http://carbontracker.noaa.gov) system (Peters et al., 2007). Carbon Tracker (CT) is based on the TM5 model, which is a global atmospheric chemistry-transport zoom model (Krol et al., 2005) optimized with highly accurate CO_2 measurements at the Earth's surface from the NOAA/ESRL network. Results have been averaged monthly for the 50° N–60° N latitude band to make comparisons with retrieved profiles from ACE-FTS for the years 2005 to 2008.

ACPD
10, 26473–26512, 2010

4.1 Monthly averaged CO_2 profiles

Figures 7–10 show model simulations (either CT alone or both CT and Flexpart) and ACE-retrieved profiles from 2005 to 2008, respectively, for the two months of May and July for the 50° N–60° N latitude band. These two months are well represented with respect to the number of occultations available and show contrasting properties in terms of atmospheric transport. Both CT and Flexpart model standard deviations are around 1 ppm and ACE-retrieved profile standard deviation is about 4 ppm for the lowest altitude and about 2–3 ppm above. Figure 7 corresponds to 2005; ACE-retrieved profiles start around 400–500 hPa in the troposphere. Comparisons with CT profiles show a good overall agreement from 400 hPa to 70 hPa with a mean difference of less than 2 ppm. ACE values in May from 180 hPa to 70 hPa are smaller than the model values by about 2 ppm (however, less than 10 occultations on average, are available). The large vertical gradient is seen by both products. In July, the ACE retrieved profile shows no vertical gradient contrary to CT that shows a "peak" of about +3 ppm at about 180 hPa with respect to the 500 hPa value. Observations from SPURT show almost no gradient in July 2002 (Hoor et al., 2004) and observations from CONTRAIL show a gradient of about 4 ppm in July and of about 3 ppm in July 2007. Both ACE and CT however agree on a gradient that is much smaller in July than in May.

Figure 8 shows Flexpart, CT and ACE-retrieved CO_2 profiles in the 50° N–60° N latitude band for the months of May and July 2006. A rather good agreement is found between these three sets of profiles. The difference is less than 2 ppm for most of the altitudes. In May, the Flexpart and CT profiles are very consistent in the troposphere whereas the difference reaches 2 ppm above the tropopause. The ACE-retrieved profile shows lower values (~ 1.5 ppm) below 300 hPa and is closer to the Flexpart profile up to 100 hPa. At higher altitudes, a significant decrease in the ACE retrieved-profile is observed, not seen by the models. Between 100 and 200 hPa, ACE is between the two models. In July, the Flexpart profile is about 1 ppm higher than the CT profile at all the altitudes. ACE is closer to CT at lower altitudes and closer to

ACPD
10, 26473–26512, 2010

Flexpart at higher altitudes. The vertical gradient is somewhat smaller for ACE than for the models.

Figure 9 shows results similar to Fig. 7 for the year 2007. The agreement between ACE-retrieved and CT simulated profiles is again good with a mean difference less than 1 ppm and gradients similar in May and slightly smaller for ACE in July. ACE-retrieved concentrations in the troposphere and higher in the stratosphere compare well with the model.

Figure 10 shows results similar to Fig. 7 for the year 2008. Here, the agreement is significantly worse with a mean difference of about 2 ppm especially above 250 hPa in May and 200 hPa in July. The difference is smaller in the troposphere. The tropopause transition is smoother for ACE in May and steeper in July where a larger ACE gradient is seen.

It must be pointed out that, for all years, the July peak value seen at about 200 hPa in CT profiles is also seen in ACE profiles but at significantly higher altitudes (except in 2006, where no peak value is seen in ACE profile).

These comparisons show that the CO_2 concentration profiles retrieved from ACE-FTS observations are quite consistent with model simulations in the northern hemisphere mid-latitudes for two particular months characterized by either a strong vertical gradient (May) or a weak (or no) gradient (July). The largest differences (~3 ppm) are observed for the latter month.

4.2 Can a temporal shift of the model profiles improve the agreement with ACE-retrieved profiles?

Current problems with air-transport models have been briefly summarized in the Introduction. These model deficiencies can cause over or under estimation of tracer profiles, with the anomalies depending on the time of year and on the altitude (troposphere or stratosphere). As a consequence, a profile retrieved at a given month might more favourably be compared with a profile simulated by the model for the month just before or just after the month considered.

ACPD
10, 26473–26512, 2010

In this section we look for such temporal shifts between model profile simulations and ACE-retrieved profiles. We examine two years: 2006 which presents the best general agreement between ACE and CT, and 2008 which corresponds to the poorest agreement.

Figure 11 shows for the 50° N–60° N latitude band, ACE-retrieved profiles for May and July 2006 together with Flexpart and CT profiles for the months just after (June and August; top row) and for the months just before (April and June; bottom row). Although the original comparison showed generally good agreement (see Fig. 8), a slight improvement is seen when comparing ACE in May to CT in June above 200 hPa and a more significant improvement in the agreement is seen when comparing ACE to both CT and Flexpart below 200 hPa (top-left). A slight degradation is observed when comparing ACE in May to both Flexpart and CT in April (bottom-left). A similar agreement is found when comparing ACE in July to both models in August, except that ACE agrees better with Flexpart below 200 hPa than with CT (top-right); a strong degradation is observed when comparing ACE in July to both Flexpart and CT in June (bottom-right).

Figure 12 shows, for the 50° N–60° N latitude band, ACE-retrieved profiles for May and July 2008 together with Flexpart profiles for the months just after (June and August; top row) and for the months just before (April and June; bottom row). Compared to Fig. 10, the ACE profile in May agrees better with the CT profile in June above 300 hPa but the fit is poorer below (top-left); the agreement is similar when comparing ACE in May to CT in April (bottom-left). Compared to Fig. 10, the ACE profile in July agrees slightly better with the CT profile in August (top-right); the agreement is much poorer when comparing ACE in May to CT in June (bottom-right).

A provisional conclusion from this very limited exercise is that ACE-retrieved profiles agree better with model profiles for the month just after the ACE month considered. More comparisons are obviously required before concluding there is deficiency in the models or possible problems with the retrievals.

ACPD
10, 26473–26512, 2010

A general agreement between model-simulated and ACE-retrieved profiles for the 50° N–60° N latitude band in May and July is evident from this comparison. However, differences are observed notably above and around the tropopause region. We also observe that comparing the ACE profile in May to model profiles in April improves the fit (mean and standard deviation) for all years considered here. The improvement is less significant in July. A strong degradation generally occurs when comparing ACE profiles in July to model profiles in June. This suggests that the model circulation strength might be over estimated during the northern hemisphere spring. Obviously, this does not exclude errors in the retrieval method and many more comparisons of retrievals vs. models are required before a convincing conclusion can be drawn.

5 Conclusions

In this paper we have presented, for the first time, five years of monthly mean CO_2 vertical profiles (5–25 km) from the ACE-FTS limb-viewing space-borne instrument (Bernath et al., 2005). After having briefly reviewed the inversion approach described in detail in Fal2009, results obtained for the 2004–2008 time period and for the 40° N–60° N and 50° N–60° N latitude bands have been compared with in situ aircraft measurements from the CONTRAIL (Machida et al., 2008), CARIBIC (Brenninkmeijer et al., 1999), and SPURT (Hoor et al., 2004) in situ aircraft measurements, as well as with two air transport model CO_2 profile simulations: Flexpart (Stohl et al., 2005) and Carbon Tracker (Peters et al., 2007). These comparisons have shown that the CO_2 concentrations retrieved from ACE-FTS are consistent with aircraft measurements in the Northern Hemisphere mid-latitudes. In particular, the mean growth rate, the seasonal vertical gradient change and phase shift from the mid-troposphere to the lower stratosphere are well represented by ACE-retrieved CO_2 values. However the stratosphere seasonal cycle amplitude (16–18 km) seems somewhat over estimated. A possible explanation could come from the difference in the spatial coverage of the different data sets. Indeed, ACE-FTS results cover all latitudes and longitudes of the

ACPD
10, 26473–26512, 2010

40° N–60° N and 50° N–60° N bands, whereas SPURT, CARIBIC, and CONTRAIL data correspond to observation above Europe, Eurasia, and Asia, respectively. Comparisons for two particular months, May (characterized by a strong vertical gradient) and July (characterized by a weak- or no-gradient) have shown that the CO_2 concentration profiles retrieved from ACE-FTS observations are quite consistent with model simulations in the Northern Hemisphere mid-latitudes. However, differences are observed notably above and around the tropopause region. Current deficiencies in air-transport models may cause over or under estimates of tracer profiles, and these anomalies depend on the time of the year and on the altitude (troposphere or stratosphere). For this reason, we looked for temporal shifts between model profile simulations and ACE-retrieved profiles and observed thatcomparing ACE profiles in May to model profiles in April improves the fit for all the years considered here. The improvement is less significant in July. A strong degradation generally occurs when comparing ACE profiles in July to model profiles in June. This suggests that the model circulation strength is over estimated during the Northern Hemisphere spring. Obviously, this does not exclude errors in the retrieval method and more comparisons are required before a firm conclusion can be drawn. Future developments include: (i) the improvement of the modelling of the N_2 continuum absorption; (ii) the processing of the years 2009 and 2010; (iii) the analysis of other latitude bands and specific geographic regions with a better space-time resolution.

This new ACE-FTS CO_2 profile database provides information on air transport and data for assimilation into models. Coupled with column measurements from a nadir viewing instrument, it may also be expected that occultation measurements will bring useful constraints to the surface carbon flux determination.

ACPD
10, 26473–26512, 2010

Appendix A

ACE retrieved monthly mean profiles from 2005 to 2007

In this appendix, Figs. A1 to A3 represent monthly averaged ACE-retrieved CO_2 profiles for the nine months available in the 50° N–60° N latitude band from 2005 to 2007.

Acknowledgements. The ACE mission is supported primarily by the Canadian Space Agency (CSA) and some support was provided by the Natural Environment Research Council (NERC) of the UK. We gratefully acknowledge J. M. Hartmann for providing us with the N_2 continuum CIA laboratory measurements and for fruitful discussions which led to their integration in our RTM. CarbonTracker 2009 results were provided by NOAA ESRL, Boulder, Colorado, USA through the website at http://carbontracker.noaa.gov. We especially wish to thank A. Jacobson and W. Peters for their help. Warm thanks are also extended to N. A. Scott and to V. Capelle for their important contributions to the development of the Radiative Transfer Model used here.

The publication of this article is financed by CNRS-INSU.

ACPD
10, 26473–26512, 2010

References

Anderson, B., Gregory, G., Collins, J. J., Sachse, G., Conway, T., and Whiting, G.: Airborne observations of spatial and temporal variability of tropospheric carbon dioxide, J. Geophys. Res., 101, 1985–1997, 1996. 26476

Bernath, P. F.: Atmospheric Chemistry Experiment (ACE): Analytical Chemistry from Orbit, TRAC-Trend. Anal. Chem., 25, 647–654, 2006. 26476, 26478

Bernath, P. F., McElroy, C. T., Abrams, M. C., Boone, C. D., Butler, M., Camy-Peyret, C., Carleer, M., Clerbaux, C., Coheur, P.-F., Colin, R., DeCola, P., DeMaziere, M., Drummond, J. R., Dufour, D., Evans, W. F. J., Fast, H., Fussen, D., Gilbert, K., Jennings, D. E., Llewellyn, E. J., Lowe, R. P., Mahieu, E., Mc-Connel, J. C., McHugh, M., Mcleod, S. D., Michaud, R., Midwinter, C., Nassar, R., Nichitiu, F., Nowland, C., Rinsland, C. P., Rochon, Y. J., Rowlands, N., Semeniuxk, K., Simon, P., Skelton, R., Sloan, J. J., Soucy, M. A., Strong, K., Tremblay, P., Turnbull, D., Walker, K. A., Walkty, I., Wardle, D. A., Wehrle, V., Zander, R., and Zou, T.: Atmospheric Chemistry Experiment (ACE): Misson overview, Geophys. Res. Lett., 32, L15S01, doi:10.1029/2005GLO22386, 2005. 26476, 26489

Bönisch, H., Hoor, P., Gurk, C., Feng, W., Chipperfield, M., Engel, A., and Bregman, B.: Model evaluation of CO_2 and SF_6 in the extratropical UT/LS region, J. Geophys. Res., 113, D06101, doi:10.1029/2007JD008829, 2008. 26475, 26483

Boone, C. D., Nassar, R., Walker, K. A., Rochon, Y., Mcleod, S. D., Rinsland, C. P., and Bernath, P. F.: Retrievals for the Atmospheric Chemistry Experiment Fourier-Transform Spectrometrer, Appl. Optics, 44, 7218–7231, 2005. 26478, 26481, 26482

Brenninkmeijer, C. A. M., Crutzen, P. J., Fischer, H., Gsten, H., Hans, W., Heinrich, G., Heintzenberg, J., Hermann, M., Immelmann, T., Kersting, D., Maiss, M., Nolle, M., Pitscheider, A., Pohlkamp, H., Scharffe, D., Specht, K., and Wiedensohler, A.: CARIBIC: Civil Aircraft for Global Measurement of Trace Gases and Aerosols in the Tropopause Region, J. Atmos. Ocean. Tech., 16, 1373–1383, 1999. 26483, 26489

Brenninkmeijer, C. A. M., Crutzen, P., Boumard, F., Dauer, T., Dix, B., Ebinghaus, R., Filippi, D., Fischer, H., Franke, H., Frieß, U., Heintzenberg, J., Helleis, F., Hermann, M., Kock, H. H., Koeppel, C., Lelieveld, J., Leuenberger, M., Martinsson, B. G., Miemczyk, S., Moret, H. P., Nguyen, H. N., Nyfeler, P., Oram, D., O'Sullivan, D., Penkett, S., Platt, U., Pupek, M., Ramonet, M., Randa, B., Reichelt, M., Rhee, T. S., Rohwer, J., Rosenfeld, K., Scharffe, D., Schlager, H., Schumann, U., Slemr, F., Sprung, D., Stock, P., Thaler, R., Valentino, F.,

ACPD
10, 26473–26512, 2010

van Velthoven, P., Waibel, A., Wandel, A., Waschitschek, K., Wiedensohler, A., Xueref-Remy, I., Zahn, A., Zech, U., and Ziereis, H.: Civil Aircraft for the regular investigation of the atmosphere based on an instrumented container: The new CARIBIC system, Atmos. Chem. Phys., 7, 4953–4976, doi:10.5194/acp-7-4953-2007, 2007. 26483

Buchwitz, M., de Beek, R., Noël, S., Burrows, J. P., Bovensmann, H., Bremer, H., Bergamaschi, P., Krner, S., and Heimann, M.: Carbon monoxide, methane and carbon dioxide columns retrieved from SCIAMACHY by WFM-DOAS: year 2003 initial data set, Atmos. Chem. Phys., 5, 3313–3329, doi:10.5194/acp-5-3313-2005, 2005. 26475

Chédin, A., Serrar, S., Armante, R., Scott, N. A., and Hollingsworth, A.: Signatures of annual and seasonal variations of $CO_2$and other greenhouse gases from comparisons between NOAA/TOVS observations and model simulations, J. Climate, 15, 95–116, 2002. 26475

Chédin, A., Scott, N. A., Crevoisier, C., and Armante, R.: First global measurement of mid-tropospheric CO_2 from NOAA polar satellites : the tropical zone, J. Geophys. Res., 108(D18), 4581, doi:10.1029/2003JD003439, 2003a. 26475

Chédin, A., Saunders, R., Hollingsworth, A., Scott, N. A., Matricardi, M., Etcheto, J., Clerbaux, C., Armante, R., and Crevoisier, C.: The feasibility of monitoring CO_2 from high-resolution infrared sounders, J. Geophys. Res., 108, 4064, doi:10.1029/2001JD00144, 2003b. 26475

Crevoisier, C., Heilliette, S., Chédin, A., Serrar, S., Armante, R., and Scott, N. A.: Midtropospheric CO_2 concentration retrieval from AIRS observations in the tropics, Geophys. Res. Lett., 31, L17106, doi:10.1029/2004GL020141, 2004. 26475

Crevoisier, C., Chédin, A., Matsueda, H., Machida, T., Armante, R., and Scott, N. A.: First year of upper tropospheric integrated content of CO_2 from IASI hyperspectral infrared observations, Atmos. Chem. Phys., 9, 4797–4810, doi:10.5194/acp-9-4797-2009, 2009. 26475

Engel, A., Bönisch, H., Brunner, D., Fischer, H., Franke, H., Gnther, G., Gurk, C., Hegglin, M., Hoor, P., Königstedt, R., Krebsbach, M., Maser, R., Parchatka, U., Peter, T., Schell, D., Schiller, C., Schmidt, U., Spelten, N., Szabo, T., Weers, U., Wernli, H., Wetter, T., and Wirth, V.: Highly resolved observations of trace gases in the lowermost stratosphere and upper troposphere from the Spurt project: an overview, Atmos. Chem. Phys., 6, 283–301, doi:10.5194/acp-6-283-2006, 2006. 26483

Foucher, P. Y., Chédin, A., Dufour, G., Capelle, V., Boone, C. D., and Bernath, P.: Technical Note: Feasibility of CO_2 profile retrieval from limb viewing solar occultation made by the ACE-FTS instrument, Atmos. Chem. Phys., 9, 2873–2890, doi:10.5194/acp-9-2873-2009,

ACPD

10, 26473–26512, 2010

2009. 26476, 26477, 26478

Foucher, P. Y.: Détermination de profils verticaux de concentration en CO_2 atmosphérique à partir d'observations spatiales. Application aux donnés en occultation solaire de l'instrument ACE-FTS sur SCISAT 1, Ph.D. thesis, University Pierre et Marie Curie, Paris, 2009 (in French). 26476, 26477, 26478, 26480

Gurk, Ch., Fischer, H., Hoor, P., Lawrence, M. G., Lelieveld, J., and Wernli, H.: Airborne in-situ measurements of vertical, seasonal and latitudinal distributions of carbon dioxide over Europe, Atmos. Chem. Phys., 8, 6395–6403, doi:10.5194/acp-8-6395-2008, 2008. 26483, 26484

Hoor, P., Gurk, C., Brunner, D., Hegglin, M. I., Wernli, H., and Fischer, H.: Seasonality and extent of extratropical TST derived from in-situ CO measurements during SPURT, Atmos. Chem. Phys., 4, 1427–1442, doi:10.5194/acp-4-1427-2004, 2004. 26483, 26484, 26486, 26489

Horowitz, L. W., Walters, S., Mauzerall, D. L., Emmons, L. K., Rasch, P. J., Granier, C., Tie, X., Lamarque, J. F., Schultz, M. G., Tyndall, G. S., Orlando, J. J., and Brasseu, G. P.: A global simulation of tropospheric ozone and related tracers: Description and evaluation of MOZART, version 2, J. Geophys. Res., 108, 4784, doi:10.1029/2002JD002853, 2003. 26480

Jacquinet-Husson, N., Scott, N. A., Chédin, A., Crépeau, L., Armante, R., Capelle, V., Orphal, J., Coustenis, A., Boonne, C., Poulet-Crovisier, N., Barbe, A., Birk, M., Brown, L. R., Camy-Peyret, C., Claveau, C., Chance, K., Christidis, N., Clerbaux, C., Coheur, P. F., Dana, V., Daumont, L., Backer-Barilly, M. R. D., Lonardo, G. D., Flaud, J. M., Goldman, A., Hamdouni, A., Hess, M., Hurley, M. D., Jacquemart, D., Kleiner, I., Kpke, P., Mandin, J. Y., Massie, S., Mikhailenko, S., Nemtchinov, V., Nikitin, A., Newnham, D., Perrin, A., Perevalov, V., Pinnock, S., Rgalia-Jarlot, L., Rinsland, C., Rublev, A., Schreier, F., Schult, L., Smithu, K. M., Tashkun, S. A., Teffo, J. L., Toth, R. A., Tyuterev, V. G., Auwera, J. V., Varanasi, P., and Wagner, G.: The GEISA spectroscopic database: Current and future archive for Earth and planetary atmosphere studies, J. Quant. Spectrosc. Ra., 100, 1043–1059, 2008. 26481

Krol, M., Houweling, S., Bregman, B., van den Broek, M., Segers, A., van Velthoven, P., Peters, W., Dentener, F., and Bergamaschi, P.: The two-way nested global chemistry-transport zoom model TM5: algorithm and applications, Atmos. Chem. Phys., 5, 417–432, doi:10.5194/acp-5-417-2005, 2005. 26485

Kuze, A., Suto, H., Nakajima, M., and Hamazaki, T.: Initial Onboard Performance of TANSO-FTS on GOSAT, in Fourier Transform Spectroscopy, OSA Technical Digest, Optical Society

ACPD

10, 26473–26512, 2010

of America, 2009. 26475
Lafferty, W. J., Solodov, A. M., Weber, A., Olson, W. B., and Hartmann, J.-M.: Infrared collision-induced absorption by N_2 near 4.3 µm for atmospheric applications: measurements and empirical modeling, Appl. Optics, 35, 5911–5917, 1996. 26477
Machida, T., Matsueda, H., Sawa, Y., Nakagawa, Y., Hirotani K., Kondo, N., Goto, K., Nakazawa, T., Ishikawa, K., and Ogawa T.: Worldwide measurements of atmospheric CO_2 and other trace gas species using commercial airlines, J. Atmos. Ocean. Tech., 25, 1744–1754, 2008. 26482, 26489
Matsueda, H., Taguchi, S., Inoue, H. Y., and Ishii, M.: A large impact of tropical biomass burning on CO and CO_2 in the upper troposphere, Science China Press, 45, 116–125, 2002. 26476, 26482
Matsueda, H., Machida, T., Sawa, Y., Nakagawa, Y., Hirotani, K., Ikeda, H., Kondo, N., and Goto, K.: Evaluation of atmospheric CO_2 measurements from new air sampling of JAL airliner observations, Pap. Meteorol. Geophys., 59, 1–17, 2008. 26482
Nakazawa, T., Miyashita, K., Aoki, S., and Tanaka, M.: Temporal and spatial variations of upper troposphere and lower stratospheric carbon dioxide, Tellus B, 43, 106–117, 1991. 26482
Niro, F., Boulet, C., and Hartmann, J.-M.: Spectra calculations in central and wing regions of CO_2 IR bands between 10 and 20 µm. I – Model and laboratory measurements, J. Quant. Spectrosc. Ra., 88, 483–498, 2004. 26478
Olsen, S. C. and Randerson, J. T.: Differences between surface and column atmospheric CO_2 and implications for carbon cycle research, J. Geophys. Res., 109, D02301, doi:10.1029/2003JD003968, 2004. 26476
Peters, W., Jacobson, A. R., Sweeney, C., Andrews, A. E., Conway, T. J., Masarie, K., Miller, J. B., Bruhwiler, L. M. P., Pétron, G., Hirsch, A. I., Worthy, D. E. J., van der Werf, G. R., Randerson, J. T., Wennberg, P. O., Krol, M. C., and Tans, P. P.: An atmospheric perspective on North American carbon dioxide exchange: CarbonTracker, P. Natl. Acad. Sci. USA, 104(48), 18925–18930, 2007. 26485, 26489
Plumb, R.: A "tropical pipe" model of stratospheric transport, J. Geophys. Res., 301, 3957–3972, 1996. 26475
Plumb, R. and Ko, M.: Interrelationships between mixing ratios of long-lived stratosphere constituents, J. Geophys. Res., 97, 10145–10156, 1992. 26475
Rinsland, C. P., Chiou, L. S., Boone, C., and Bernath, P.: Carbon dioxide retrievals from Atmospheric Chemistry Experiment solar occultation measurements, J. Geophys. Res., 115,

ACPD
10, 26473–26512, 2010

D03105, doi:10.1029/2009JD012081, 2010. 26478
Sawa, Y., Machida, T., and Matsueda, H.: Seasonal variations of CO_2 near the tropopause observed by commercial aircraft, J. Geophys. Res., 113, D23301, doi:10.1029/2008JD010568, 2008. 26484, 26503
Schuck, T. J., Brenninkmeijer, C. A. M., Slemr, F., Xueref-Remy, I., and Zahn, A.: Greenhouse gas analysis of air samples collected onboard the CARIBIC passenger aircraft, Atmos. Meas. Tech., 2, 449–464, doi:10.5194/amt-2-449-2009, 2009. 26483
Scott, N. A. and Chédin, A.: A fast line-by-line method for atmospheric absorption computation: The Automatized Atmospheric Absorption Atlas, J. Appl. Meteorol., 20, 801–812, 1981. 26480
Shia, R. L., Liang, M. C., Miller, C. E., and Yung, Y. L.: CO_2 in the upper troposphere: Influence of stratospheretroposphere exchange, Geophys. Res. Lett., 33, L1481, doi:10.1029/2006GL026141, 2006. 26475, 26476
Stohl, A., Forster, C., Frank, A., Seibert, P., and Wotawa, G.: Technical note: The Lagrangian particle dispersion model FLEXPART version 6.2, Atmos. Chem. Phys., 5, 2461–2474, doi:10.5194/acp-5-2461-2005, 2005. 26485, 26489
Tikhonov, A. N.: On the regularization of ill-posed problems, Dokl. Akad. Nauk SSSR, 153, 49–52; MR, 28, 5577; Soviet Math. Dokl., 4, 1624–1627, 1963. 26480

ACPD
10, 26473–26512, 2010

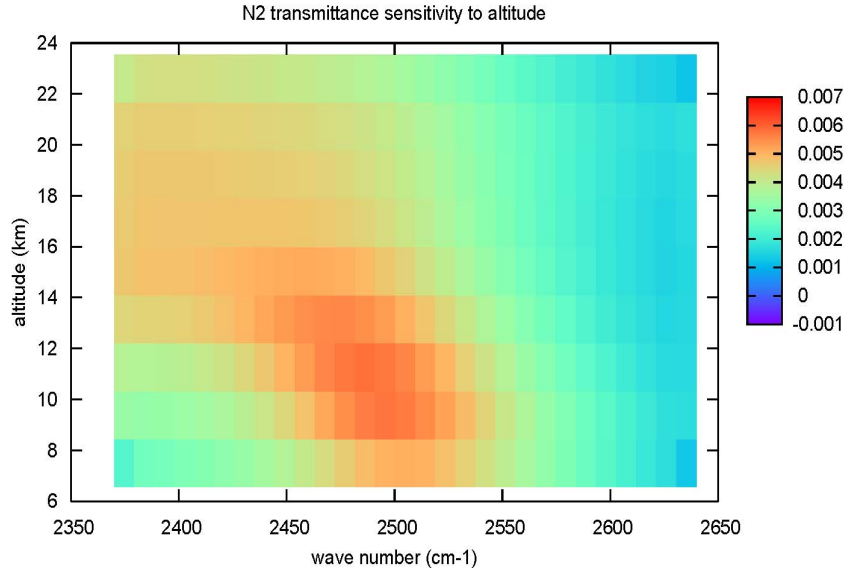

Fig. 1. Transmittance sensitivity to tangent height in the N_2 collision-induced absorption (2370–2640 cm^{-1}) spectral range. The color bar values represent the transmission variation due to a 100 m tangent height change.

ACPD
10, 26473–26512, 2010

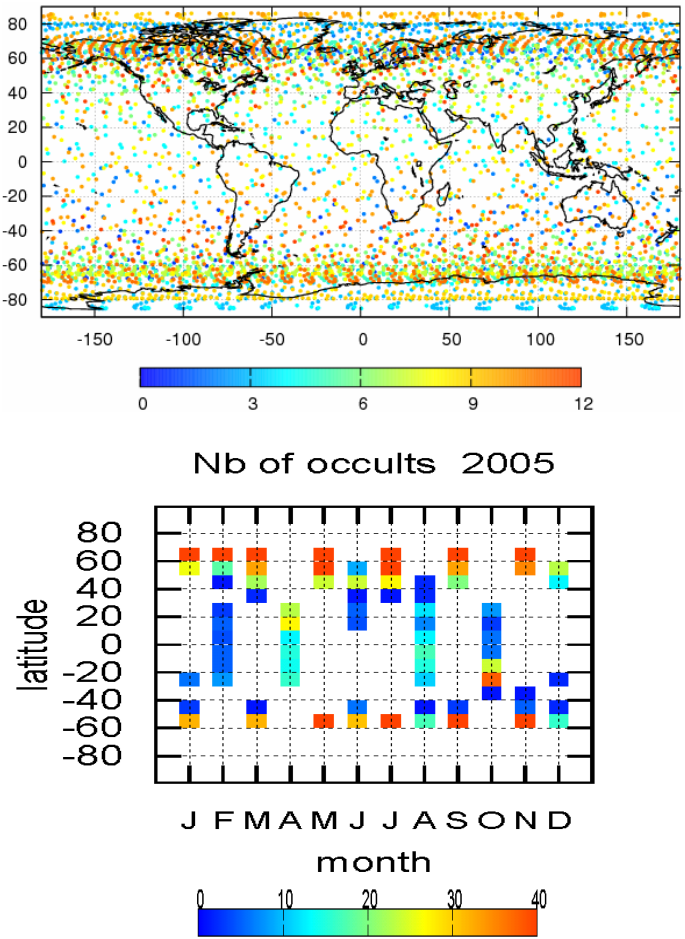

Fig. 2. Locations of ACE-FTS occultations available in 2005 per month (color scale) (top); monthly distribution of the number of occultations per 10° latitude band (bottom).

ACPD
10, 26473–26512, 2010

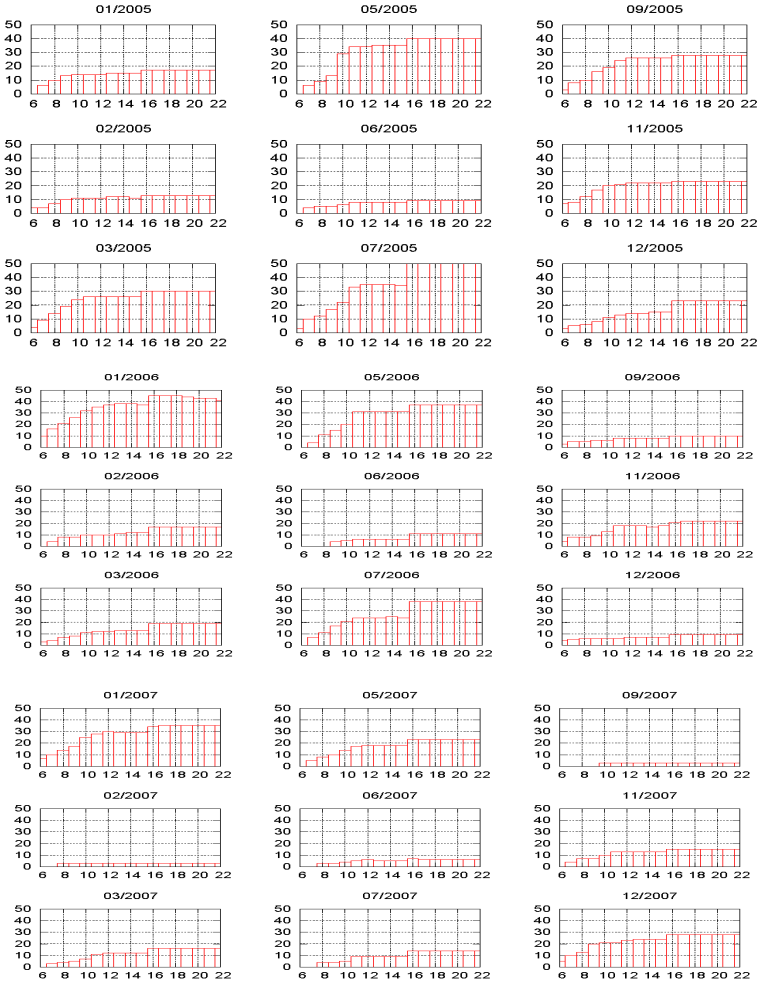

Fig. 3. Number of ACE-FTS occultations (y-axis) available for the 50° N–60° N latitude band for nine months of the years 2005 to 2007 (April, August and September are not covered for this latitude band) and for each altitude (x-axis).

ACPD
10, 26473–26512, 2010

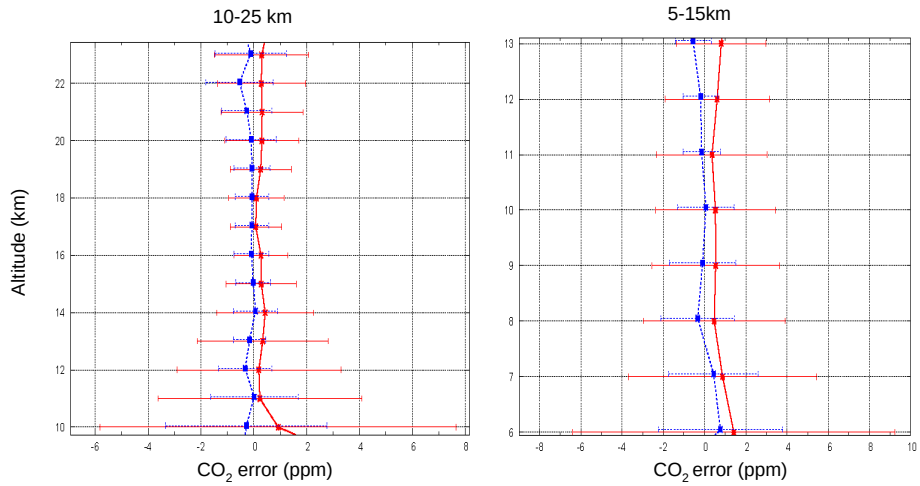

Fig. 4a. Results of synthetic retrievals of the CO_2 mixing ratio difference (in ppm) between the true profile and the retrieved profile (average over 20 occultations). Blue curve: all the uncertainties are considered as Gaussian random noise added to the "observations"; red curve: realistic temperature and species (N_2O, O_3, etc.) uncertainties are introduced in the atmospheric model; horizontal bars are one standard deviation.

ACPD
10, 26473–26512, 2010

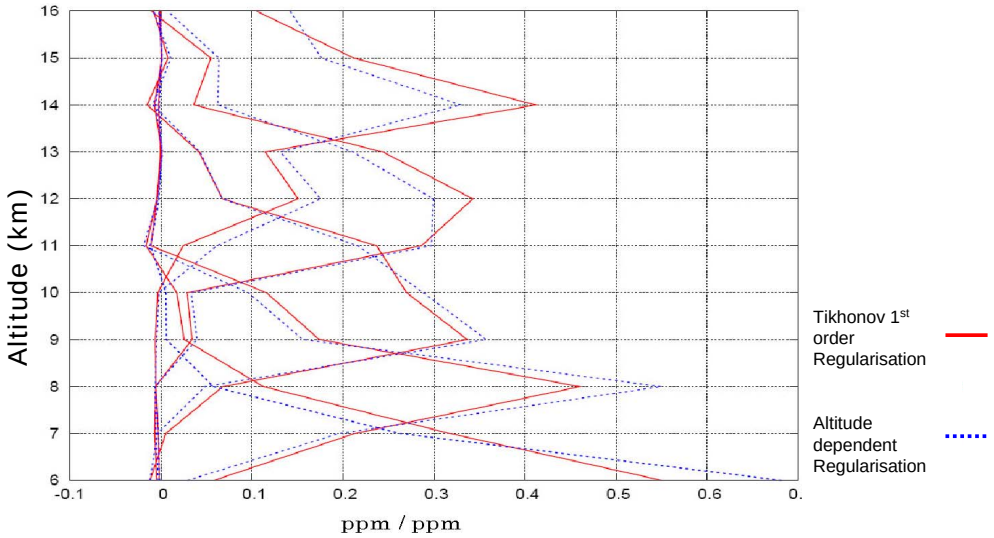

Fig. 4b. Averaging kernels for levels at 6, 8, 10, 12 and 14 km for one occultation. The red curve corresponds to a first order Tikhonov regularisation and the blue curve to an altitude dependent regularisation based on a Tikhonov first order operator.

ACPD
10, 26473–26512, 2010

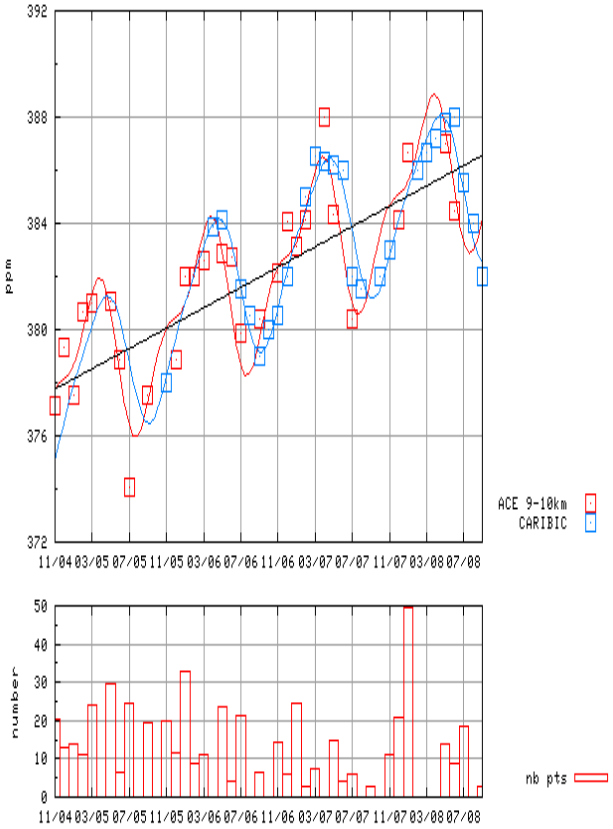

Fig. 5. Top: temporal evolution of CO_2 concentration (y-axis in ppm) in the upper troposphere (9–10 km). Blue boxes: ACE-FTS results for the 40° N–60° N latitude band; red boxes: CARIBIC measurements. The blue and red lines result from a curve fit using a harmonic polynomial (two harmonics). The slope of the best fit line corresponds to the mean growth rate during this time period: 1.9 ppm yr^{-1}. Bottom: number of ACE-FTS occultations used in the 9–10 km altitude range.

ACPD
10, 26473–26512, 2010

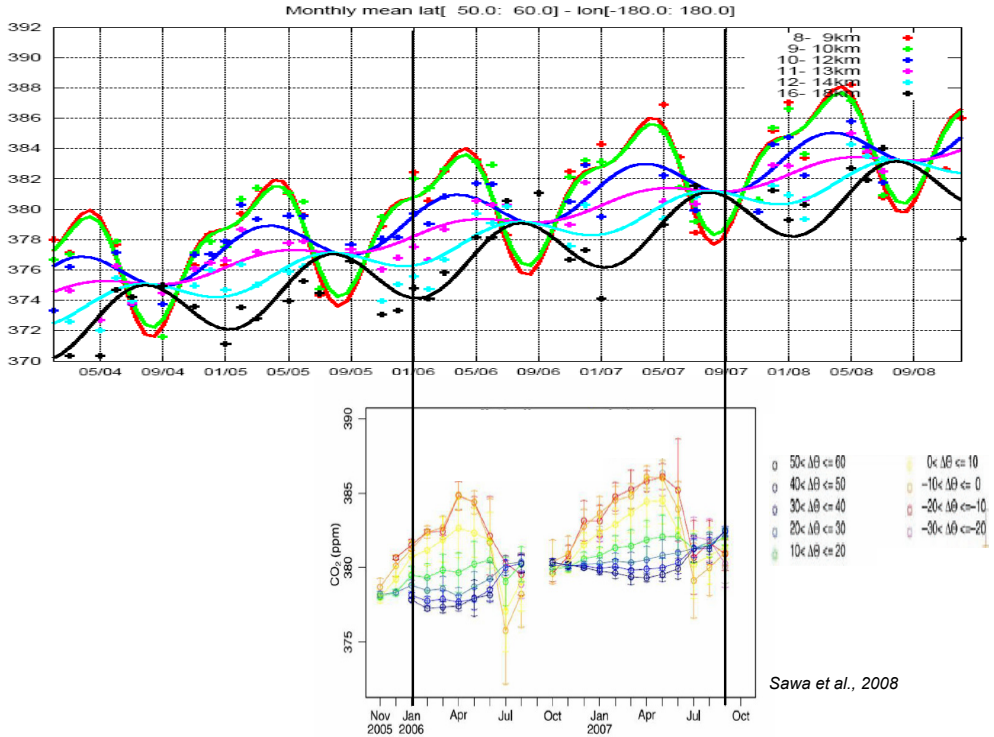

Fig. 6. Top: temporal evolution of CO_2 concentration retrieved from ACE-FTS measurements for six atmospheric layers from 8 to 18 km (see color legend). Crosses show the retrievals (monthly mean) and the curves result from the harmonic polynomial fit (two harmonics for the first two layers, one for the remaining four) to the retrievals at different altitudes. Bottom: temporal evolution of CO_2 concentration from CONTRAIL measurements (Sawa et al., 2008) above Eurasia from November 2005 to September 2007. Each curve represents CO_2 time series observed at 10 K potential temperature bins from the local tropopause. Blue curves correspond to the lower stratosphere and orange curves to the higher troposphere.

ACPD
10, 26473–26512, 2010

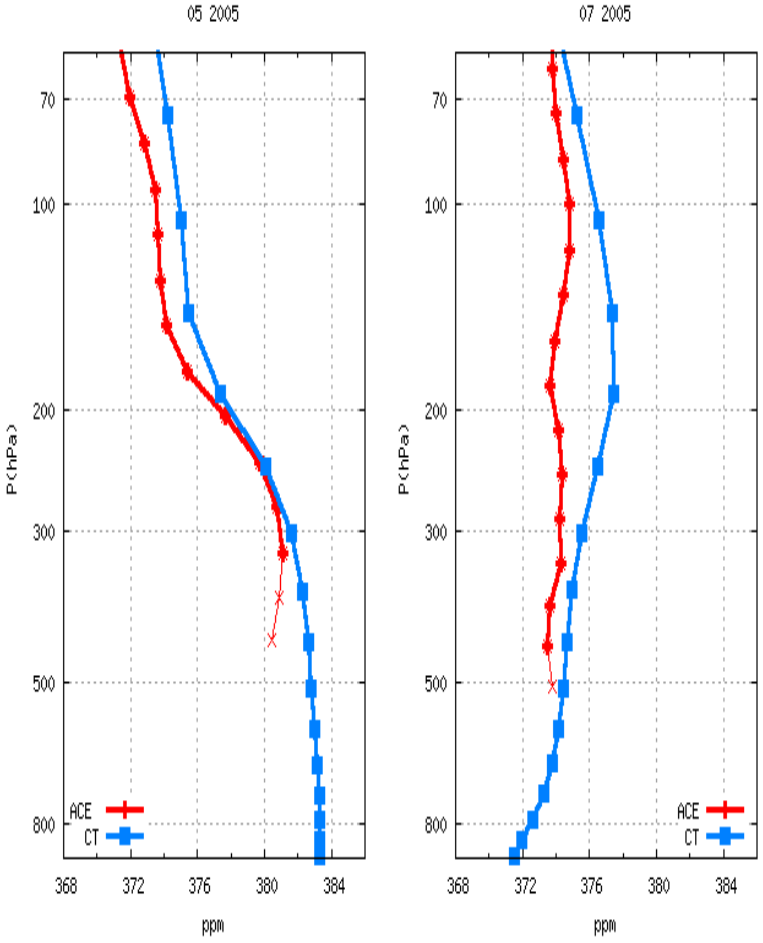

Fig. 7. CO_2 concentration (x-axis in ppm) evolution with pressure (y-axis in hPa) for May (left) and July (right) for 2005 for the 50° N–60° N latitude band. ACE-retrieved profile is in red and CT profile is in blue.

ACPD
10, 26473–26512, 2010

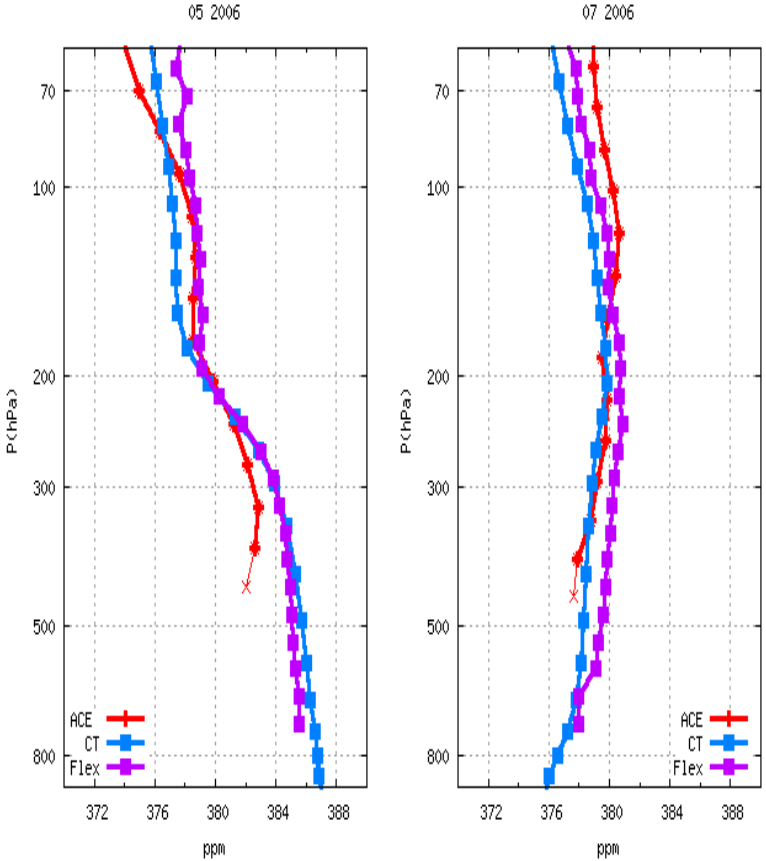

Fig. 8. CO_2 concentration (x-axis in ppm) evolution with pressure (y-axis in hPa) for May (left) and July (right) of 2006 for the 50° N–60° N latitude band. ACE-retrieved profile is in red, CT profile is in blue and Flexpart profile is in purple.

ACPD
10, 26473–26512, 2010

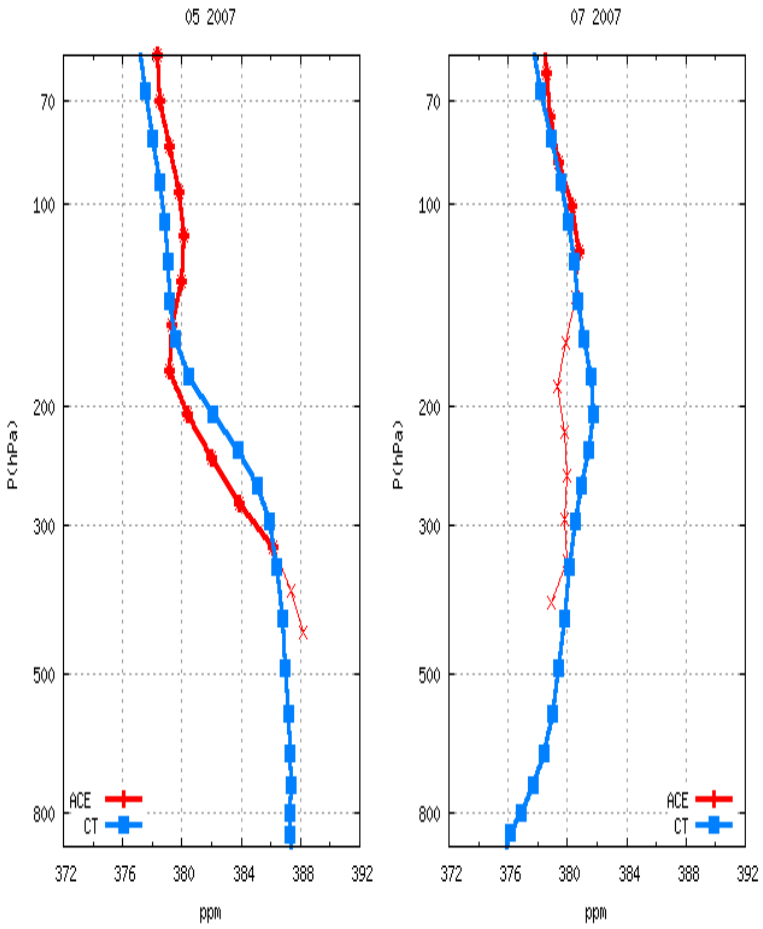

Fig. 9. Same as Fig. 7 for 2007. The thin red line indicates that less than 10 occultations were available.

ACPD
10, 26473–26512, 2010

CO_2 atmospheric profiles retrieved from space observation

P. Y. Foucher et al.

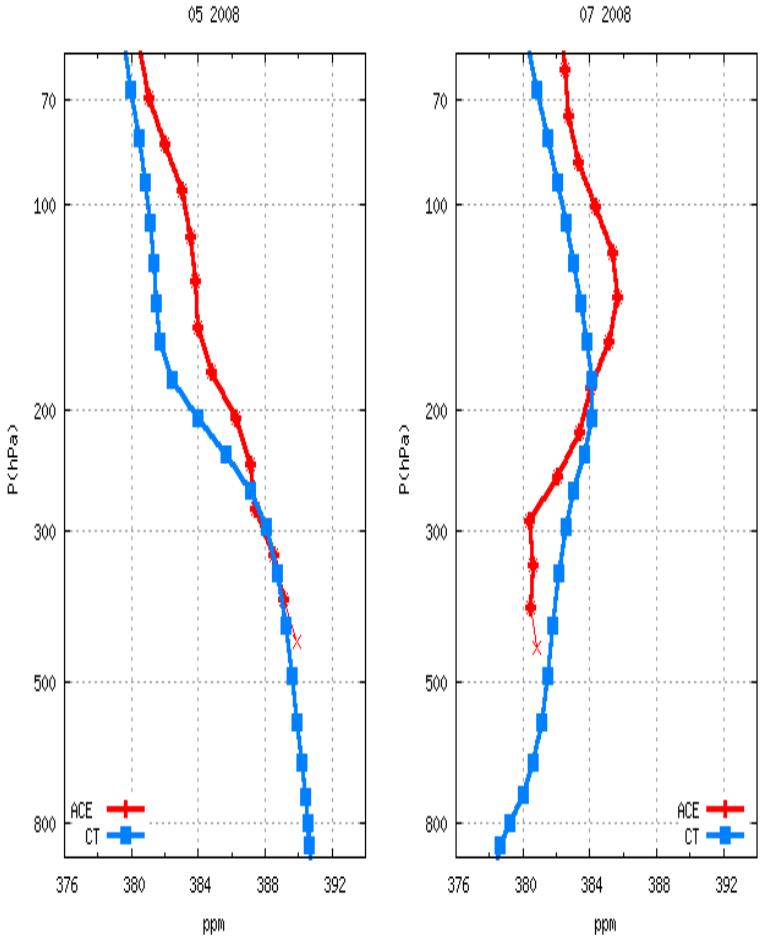

Fig. 10. Same as Fig. 7 for the year 2008.

ACPD
10, 26473–26512, 2010

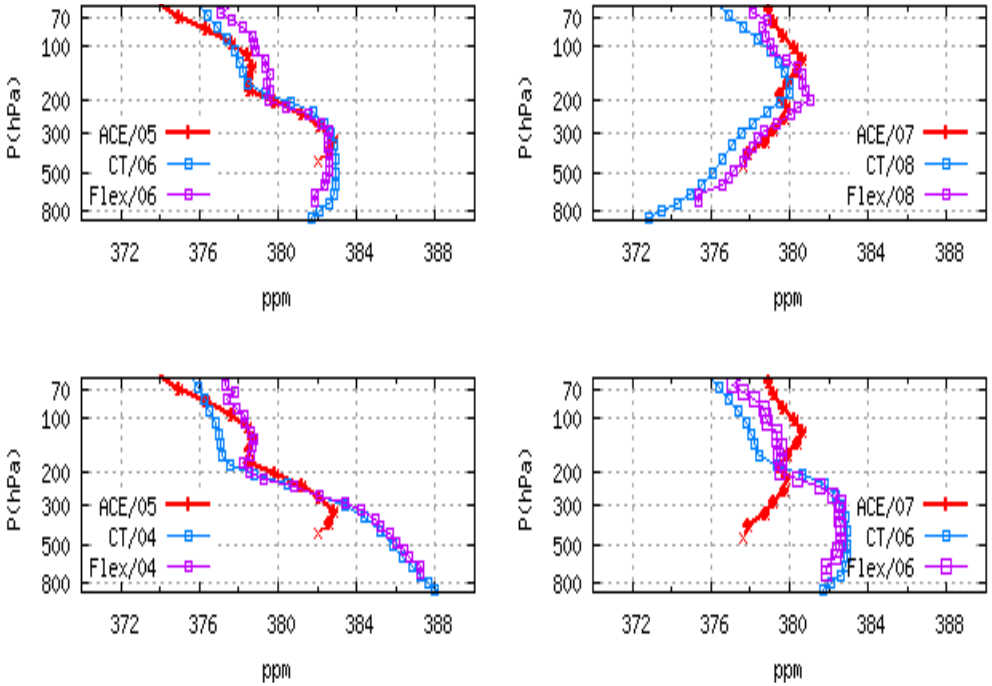

Fig. 11. Flexpart (purple), CT (blue), and ACE (red) CO_2 profiles for the 50° N–60° N latitude band in 2006. ACE profiles in May (left) and July (right) are compared to Flexpart and CT profiles of one month before (top), and of one month after (bottom).

ACPD
10, 26473–26512, 2010

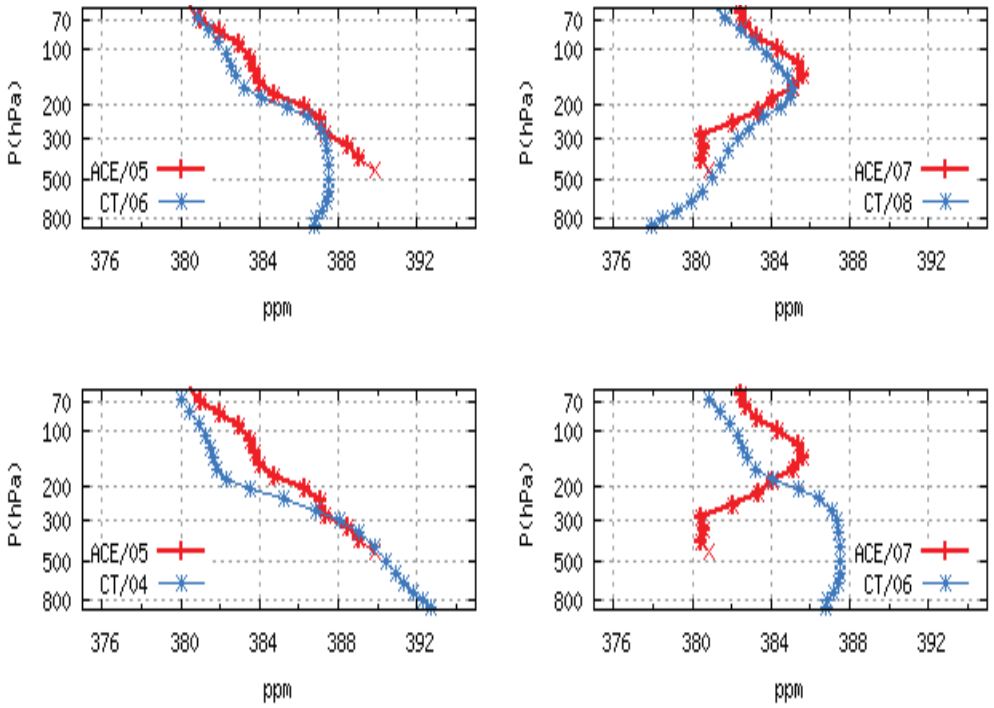

Fig. 12. CT (blue) and ACE (red) CO_2 profiles for the 50° N–60° N latitude band in 2008. ACE profiles in May (left) and July (right) are compared to CT profiles of one month before (top), and of one month after (bottom).

ACPD
10, 26473–26512, 2010

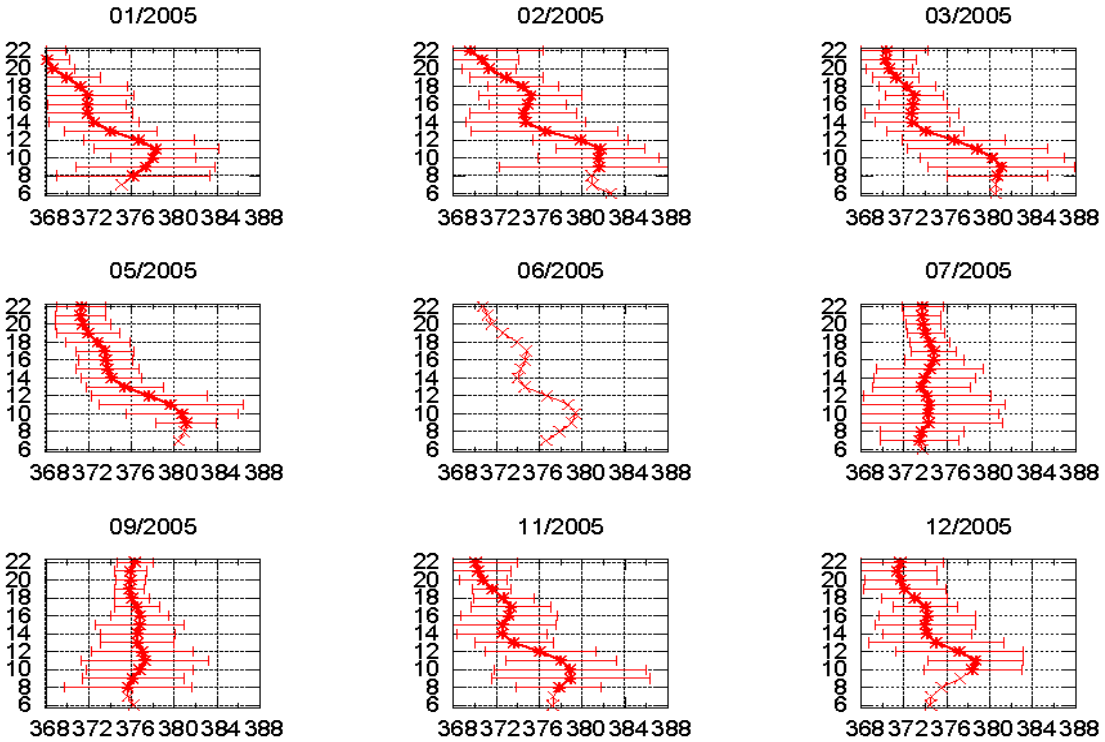

Fig. A1. Monthly mean CO_2 concentration (x-axis in ppm) evolution with altitude (y-axis in km) for nine months of 2005 for the 50° N–60° N latitude band.

ACPD
10, 26473–26512, 2010

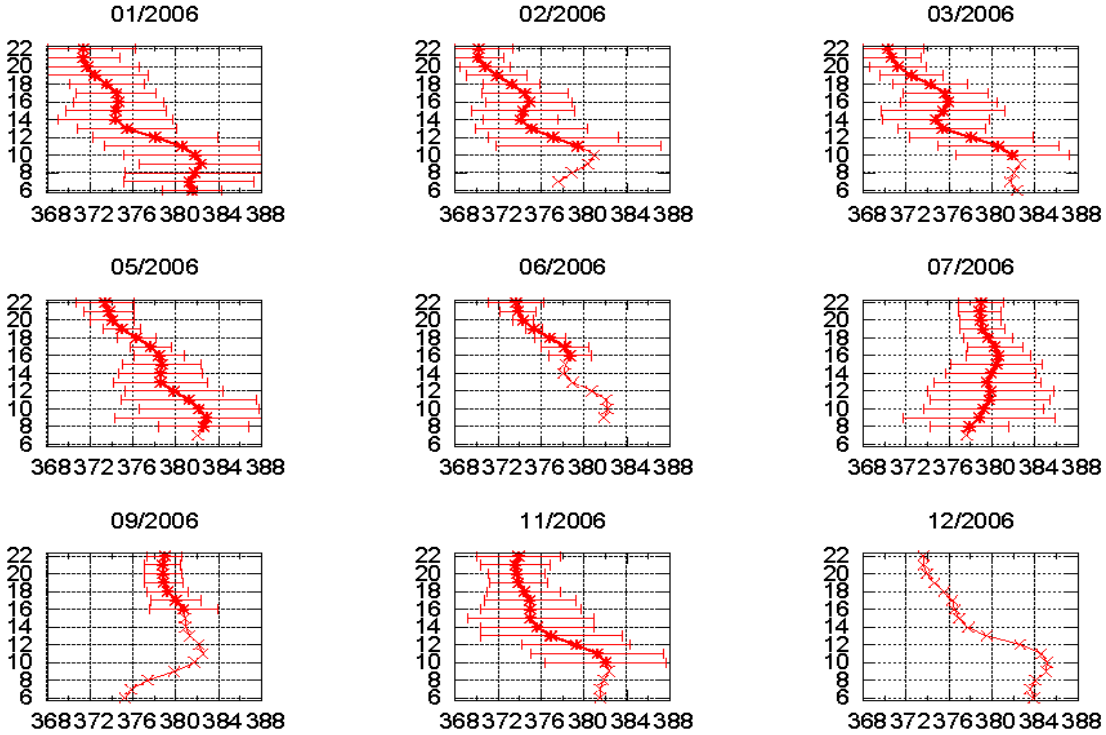

Fig. A2. Same as Fig. A1 for 2006.

ACPD
10, 26473–26512, 2010

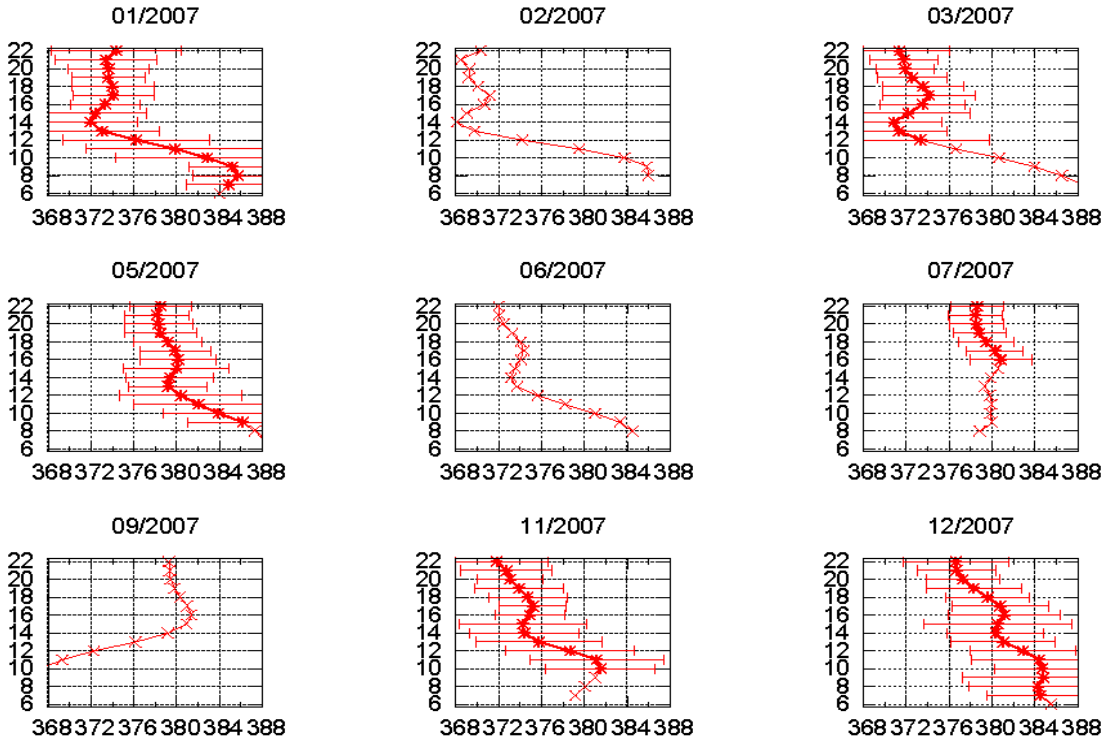

Fig. A3. Same as Fig. A1 for 2007.

ACPD
10, 26473–26512, 2010